A Human Transferrin-Vascular Endothelial Growth Factor (hnTf-VEGF) Fusion Protein Containing an Integrated Binding Site for ^{111}In for Imaging Tumor Angiogenesis

Conrad Chan, PhD[1]; Jasbir Sandhu, PhD[1]; Abhijit Guha, MD, MSc[2]; Deborah A. Scollard, BAppSci[1]; Judy Wang, MSc[1]; Paul Chen, PhD[1]; Karen Bai, DDS[3]; Lydia Lee, PhD[4]; and Raymond M. Reilly, PhD[1,5,6]

[1]Leslie Dan Faculty of Pharmacy, University of Toronto, Toronto, Ontario, Canada; [2]Arthur and Sonia Labatt Brain Tumor Research Center, The Hospital for Sick Children, Toronto, Ontario, Canada; [3]Samuel Lunenfeld Research Institute, Mount Sinai Hospital, Toronto, Ontario, Canada; [4]Transplant Research Division, Toronto General Hospital Research Institute, University Health Network, Toronto, Ontario, Canada; [5]Department of Medical Imaging, University of Toronto, Toronto, Ontario, Canada; and [6]Department of Pharmaceutical Sciences, University of Toronto, Toronto, Ontario, Canada

Our objective was to synthesize a recombinant protein (hnTf-VEGF [VEGF is vascular endothelial growth factor]) composed of $VEGF_{165}$ fused through a flexible polypeptide linker $(GGGGS)_3$ to the n-lobe of human transferrin (hnTf) for imaging angiogenesis. The hnTf domain allowed labeling with ^{111}In at a site remote from the VEGF receptor-binding domain. **Methods:** DNA encoding hnTf, peptide linker $(GGGGS)_3$, and $VEGF_{165}$ genes were cloned into the *Pichia pastoris* vector pPICZαB to generate the pPICZαB-hnTF-VEGF plasmid. The expression vector was transformed into *P. pastoris* KM71H strain. The protein was purified using Co^{2+} metal affinity resin. The growth-stimulatory effects of hnTf-VEGF on human umbilical vascular endothelial cells (HUVECs) and its binding to porcine aortic endothelial cells (PAECs) transfected with VEGF receptors were evaluated. hnTf-VEGF protein was labeled with $^{111}InCl_3$ in 10 mmol/L HEPES/15 mmol/L $NaHCO_3$ buffer, pH 7.4 (HEPES is *N*-(2-hydroxyethyl)piperazine-*N*′-(2-ethanesulfonic acid). The loss of ^{111}In in vitro from ^{111}In-hnTf-VEGF to transferrin in human plasma and to diethylenetriaminepentaacetic acid (DTPA) in buffer was determined. Tumor and normal tissue distributions of ^{111}In-hnTf-VEGF were evaluated in athymic mice implanted subcutaneously with U87MG human glioblastoma xenografts. Tumor imaging was performed. **Results:** Sodium dodecylsulfate–polyacrylamine gel electrophoresis under reducing and nonreducing conditions showed bands for hnTf-VEGF monomer (M_r of 65 kDa) and dimer (M_r of 130 kDa). hnTf-VEGF stimulated the growth of HUVECs 3-fold and demonstrated binding to PAECs displaced by a 50-fold excess of $VEGF_{165}$ but not by apotransferrin. There was 21.3% ± 3.4% loss of ^{111}In per day from ^{111}In-hnTf-VEGF to transferrin in plasma, but <5% loss to DTPA over 4 h. ^{111}In-hnTf-VEGF accumulated in U87MG tumors (6.7% injected dose per gram at 72 h after injection) and its tumor uptake decreased 15-fold by coadministration of a 100-fold excess of VEGF but not by apotransferrin. The tumor-to-blood ratio was 4.9:1 at 72 h after injection and tumors were imaged at 24–72 h after injection. **Conclusion:** ^{111}In-hnTf-VEGF is a promising radiopharmaceutical for imaging tumor angiogenesis and represents a prototypic protein harboring the metal-binding site of transferrin for labeling with ^{111}In without introducing DTPA metal chelators.

Key Words: vascular endothelial growth factor; transferrin; angiogenesis; ^{111}In; glioblastomas

J Nucl Med 2005; 46:1745–1752

Angiogenesis, the formation of new blood vessels in tumors, relieves the restriction on growth that would otherwise exist because of the limited diffusion distance of oxygen and nutrients (only a few millimeters) from the vessels. Angiogenesis represents one of the key molecular "switches" that permit progression of cancer and allow its invasion into the surrounding stroma, which may lead to metastasis (*1*). Solid tumors such as glioblastomas are highly vascularized due to secretion of vascular endothelial growth factor (VEGF) by tumor cells that promotes angiogenesis by stimulating the growth of vascular endothelial cells (VECs) (*2,3*). Furthermore, VEGF secretion increases in a paracrine fashion the expression of its cognate receptors, VEGFR1 and VEGFR2 (also known as flt-1 and Kinase insert Domain containing Receptor—KDR or flk-1), on tumor VECs. In contrast, nonstimulated and quiescent VECs exhibit low levels of VEGFRs (*4,5*). Because of its pivotal role in tumor progression, angiogenesis presents a highly attractive target for therapeutic intervention (*6*).

It would be useful to have radiopharmaceuticals that could noninvasively assess the extent of tumor angiogenesis by imaging the expression of VEGFRs on the vasculature.

Received Dec. 15, 2004; revision accepted Jul. 13, 2005.

For correspondence or reprints contact: Raymond M. Reilly, PhD, Leslie Dan Faculty of Pharmacy, University of Toronto, 19 Russell St., Toronto, Ontario, Canada.

E-mail: raymond.reilly@utoronto.ca

Imaging of tumor VEGFR expression may predict the effectiveness or monitor the response to novel antiangiogenic therapy in cancer patients. One candidate for constructing radiopharmaceuticals for imaging VEGFR expression may be VEGF itself conjugated to a γ-emitting radionuclide such as ^{111}In. However, VEGF is rapidly eliminated from the blood by renal excretion with a terminal half-life of 4.75 h (*7*) due to its relatively low molecular weight (M_r of 40–46 kDa). Furthermore, conjugation to metal chelators, such as diethylenetriaminepentaacetic acid (DTPA), for labeling with ^{111}In may affect its affinity for binding VEGFR. DTPA dianhydride, which reacts with the N-terminus or ϵ-amino groups of lysines on proteins, is the most commonly used bifunctional chelator for biomolecules. $VEGF_{165}$ contains several lysines with one (Lys-84 within the β5 loop) particularly required for binding to its receptor (*8*). Derivatization of lysines critical for receptor recognition may, therefore, diminish the receptor-binding affinity of VEGF. In this report, we describe the construction, expression, and characterization of a novel recombinant protein consisting of $VEGF_{165}$ fused through a flexible polypeptide linker to the n-lobe of human transferrin (hnTf-VEGF). The dimeric hnTf-VEGF protein has a 3-fold higher molecular weight (M_r of 130 kDa) than VEGF. It binds ^{111}In at a site remote from the VEGFR-binding region through the transferrin domain without the need to introduce DTPA metal chelators. Binding of ^{111}In-hnTf-VEGF to transferrin receptors was not expected as both the n- and c-lobes are required for receptor recognition and single lobes have very limited receptor-binding capability (*9,10*). The tumor and normal tissue localization properties of ^{111}In-labeled hnTf-VEGF were evaluated in athymic mice implanted subcutaneously with highly vascularized U87MG glioblastoma xenografts.

MATERIALS AND METHODS

Construction of Plasmids Expressing hnTf-VEGF

The hnTf gene was amplified from plasmid pBluescript SK(−)-hnTf (provided by Prof. Ross T.A. MacGillivray, University of British Columbia, Vancouver) by polymerase chain reaction (PCR) (Fig. 1) using the forward hnTf primer containing a *Sac* I restriction site (italicized) GCC *GAG CTC* GGA TGG TCC CTG ATA AAA CTG TGA GA and reverse hnTf-linker primer containing a *Spe* I restriction site (italicized) and $(GGGGS)_3$ linker sequence CGC *ACT AGT* AGA TCC GCC GCC ACC CGA CCC ACC ACC GCC CGA GCC ACC GCC ACC ATC TGT TGG GGC TTC TGG. The VEGF gene was amplified from plasmid pCR2.1-VEGF (American Type Culture Collection) by PCR (Fig. 1) using the forward VEGF primer containing a *Spe* I restriction site (italicized) GCC *ACT AGT* GCA CCC ATG GCA GAA GGA GGA and reverse VEGF primer containing an *Eco*RV restriction site (italicized) CGG *GAT ATC* CCG CCT CGG CTT GTC ACA TCT (ACGT Corp.).

The amplified hnTf gene containing the linker sequence and the amplified VEGF gene were cut with corresponding restriction enzymes, ligated into pCR2.1 vector to form pCR2.1-hnTf-VEGF, and then transformed into *Escherichia coli* DH5α-strain. Plasmid DNA was prepared and the sequence of the hnTf-VEGF gene was confirmed. The pCR2.1-hnTf-VEGF was cut with *Kpn* I and *Xba* I enzymes and ligated into plasmid pPICZαB at the *Kpn* I and *Xba* I sites to produce the final expression vector pPICZαB-hnTf-VEGF (Fig. 1). This plasmid was transformed into *E. coli* strain TOP10 for large-scale preparation of the plasmid DNA. It was sequenced to confirm the correct insertion of the hnTf-VEGF gene.

Transformation of *P. pastoris*

Three micrograms of pPICZαB-hnTf-VEGF or parent pPICZαB (control) expression vectors were linearized using *Pme* I restriction enzyme (Fig. 1) and transformed into *P. pastoris* strain X33, GS115, or KM71H by the spheroplast method (Invitrogen). Transformed yeasts were selected on yeast extract peptone dextrose (YPDS) plates with Zeocin (Invitrogen).

Expression and Purification of hnTf-VEGF

Biomass from a single colony of yeast transformant was generated in buffered minimal glycerol yeast extract (BMGY) medium and resuspended in buffered minimal methanol yeast extract (BMMY) medium to induce protein expression. The expression plasmid included an α-factor secretion signal sequence that allowed the protein expressed to be directed into the medium. The growth medium was collected up to 4 d, filtered, and dialyzed (Fisher Scientific) against 50 mmol/L NaH_2PO_4 buffer, pH 7.0, in 300 mmol/L NaCl. hnTf-VEGF fusion protein was purified from

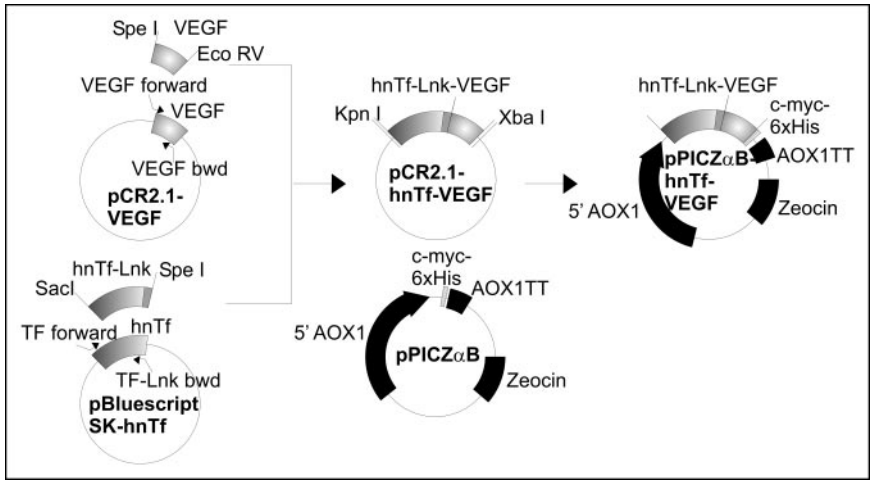

FIGURE 1. Schematic representation of generation of *P. pastoris* expression vector pPICZαB-hnTf-VEGF. TF = hnTf; bwd = backward; Lnk = linker.

the medium by mixing with Talon Co^{2+} metal affinity resin (Clontech) at room temperature for 30 min. The resin mixture was transferred to an Econo-Pac minicolumn (BioRad) and the hnTf-VEGF fusion protein was eluted using 50 mmol/L sodium acetate buffer, pH 5.0, in 300 mmol/L NaCl. Fractions containing the hnTf-VEGF fusion protein were identified by sodium dodecylsulfonate–polyacrylamide gel electrophoresis (SDS–PAGE) on a 10% Tris-HCl gel (BioRad) and Western blot using mouse anti-histidine monoclonal antibodies (Invitrogen), goat anti-VEGF or anti-TF antibodies (Sigma). These fractions were pooled and dialyzed against 50 mmol/L NaH_2PO_4 buffer, pH 5.0, in 100 mmol/L NaCl at 4°C for 16 h and then dialyzed against 10 mmol/L (HEPES) buffer, pH 7.4 (HEPES is *N*-(2-hydroxyethyl)piperazine-*N*′-(2-ethanesulfonic acid), in 15 mmol/L $NaHCO_3$ at 4°C for 16 h. The purity of hnTf-VEGF was confirmed by SDS–PAGE and Western blot.

Endothelial Cell Proliferation Assay

The biologic activity of hnTf-VEGF was evaluated in a proliferation assay using VEGFR-positive human umbilical vascular endothelial cells (HUVECs). HUVECs were grown in 96-well plate (Corning) at 5×10^3 cells per well for 48 h using Clonetics EGM-2-Endothelial Cell Medium-2 containing EGM-2 Bullet kit supplements (Cambrex). The cells were starved in 1:20 diluted growth medium 24 h before the assay, then rinsed once with diluted growth medium, and incubated with hnTf-VEGF (0.02–2.67 nmol/L) or VEGF (0.07–2.17 nmol/L) in medium or with medium alone for 72 h. Cell proliferation was determined colorimetrically using the CellTiter 96 AQueous One Solution proliferation assay (Promega). Reagent (20 μL) was added to the wells and incubated for 4 h at 37°C and 5% CO_2. The absorbance at 490 nm was measured by a plate reader (ULX-808UV; BioTek).

Evaluation of Receptor-Binding Properties by Flow Cytometry

The receptor-binding properties of hnTf-VEGF were evaluated by flow cytometry using porcine aortic endothelial cells (PAECs) transfected with the VEGFR gene or PAECs without transfection (both cell lines were provided by Dr. Lena Claesson-Welsh, Uppsala University, Uppsala, Sweden). PAECs were cultured in HAM's F12 medium with 10% fetal calf serum (FCS). Flow cytometry was performed by incubating 1×10^5 PAECs with fluorescein isothiocyanate–labeled hnTf-VEGF (5 μg/mL) in the dark at 4°C for 30 min. The cells were washed twice with phosphate-buffered saline (PBS), fixed in PBS containing 2% formaldehyde, and analyzed on a FACScan (Becton Dickinson Bioscience) flow cytometer.

Radiolabeling of hnTf-VEGF with ^{111}In

hnTf-VEGF and apotransferrin were labeled with ^{111}In by adding 6 MBq of $^{111}InCl_3$ (MDS Nordion) to 50 μg of protein in 10 mmol/L HEPES/15 mmol/L $NaHCO_3$, pH 7.4, buffer and incubating at room temperature for 1 h. ^{111}In-hnTf-VEGF or ^{111}In-apotransferrin were purified from free ^{111}In on a P-2 minicolumn eluted with 10 mmol/L HEPES/15 mmol/L $NaHCO_3$ buffer, pH 7.4. Fractions (100 μL) were collected and counted in a γ-counter (Cobra II; Packard Instruments). To exclude the possibility of binding ^{111}In through the His_6 affinity tag incorporated into hnTf-VEGF, 500 μg of an 11-mer peptide containing this sequence [GGGGSHHHHHH] (Advanced Protein Technology Centre, The Hospital for Sick Children, Toronto) in 50 μL of 10 mmol/L HEPES/15 mmol/L $NaHCO_3$ buffer, pH 7.4, were incubated for 30 min at room temperature with 1.5 MBq (5 μL) of $^{111}InCl_3$. A control labeling experiment consisted of buffer (without peptide) incubated with $^{111}InCl_3$. The percentage of ^{111}In bound to the peptide was determined by analyzing 55 μL (1.5 MBq) of the mixture on a C_{18} Sep-Pak column (Waters), eluted first with 10 mL of HEPES/$NaHCO_3$ buffer, pH 7.4, to elute free ^{111}In and eluted then with 10 mL of methanol to elute the peptide. Both fractions were measured in a radioisotope calibrator (CRC-12; Capintec).

In Vitro Stability of ^{111}In-hnTf-VEGF

The loss of ^{111}In from ^{111}In-hnTf-VEGF in vitro to transferrin was evaluated by incubation of ^{111}In-hnTf-VEGF (110 kBq/μg) with human plasma at a concentration of 15 kBq/μL for up to 72 h at 37°C. Samples were analyzed in triplicate at 4, 24, 48, and 72 h by size-exclusion high-performance liquid chromatography (HPLC) on a Beckman Gold System fitted with a BioSep SEC-S2000 column (exclusion limit, 1,000–300,000 kDa; Phenomenex) eluted with 100 mmol/L NaH_2PO_4 buffer, pH 7.0, at a flow rate of 0.7 mL/min and interfaced to a Beckman model 171 flow-through radioactivity detector. The retention time (t_R) on this system for ^{111}In-transferrin was 9.9 min determined by analysis of a sample of $^{111}InCl_3$ (2 MBq) mixed with human plasma for 4 h at 37°C. The t_R for ^{111}In-hnTf-VEGF was 8.7 min. The stability of ^{111}In-hnTf-VEGF was further examined by incubating 0.25 nmol of ^{111}In-hnTf-VEGF with 0.25 nmol of DTPA (Sigma) in 10 mmol/L HEPES/15 mmol/L $NaHCO_3$ buffer, pH 7.4, at 37°C for 4 h. The percentage of ^{111}In-DTPA (M_r of 468 Da) versus ^{111}In-hnTf-VEGF (M_r of 130 kDa) was measured by ultrafiltration through Microcon YM-50 devices (M_r cutoff, 50 kDa; Amicon).

Tumor and Normal Tissue Distributions

U87MG human glioblastoma cells (American Type Culture Collection) were cultured in Dulbeco's Modified Eagle's Medium (DMEM; Sigma) supplemented with 10% FCS. Cells (5×10^6 cells in DMEM without FCS) were inoculated subcutaneously into the hind leg of 4- to 6-wk-old female athymic (*nu/nu*) mice to establish U87MG xenografts (1- to 2-cm diameter). The mice were injected intravenously (tail vein) with 1–2 MBq (5 μg) of ^{111}In-hnTf-VEGF, ^{111}In-hnTf-VEGF mixed with a 100-fold molar excess (291 μg) of apotransferrin, or ^{111}In-hnTf-VEGF mixed with a 100-fold molar excess (171 μg) of VEGF. Groups of 3 or 4 mice were sacrificed by cervical dislocation at 48 or 72 h after injection of ^{111}In-hnTf-VEGF. The tumor and samples of normal tissues, including blood, were obtained and weighed, and their radioactivity was measured in a γ-counter. The concentration of radioactivity in the tumor and other tissues was expressed as the percentage injected dose per gram (% ID/g). In a separate experiment, the normal tissue distribution of ^{111}In-labeled transferrin was determined in a group of 3 athymic mice. Posterior, whole-body images of selected mice were obtained at 24, 48, and 72 h after injection of ^{111}In-hnTf-VEGF on an Elscint SP4 single-head γ-camera fitted with a 4-mm pinhole collimator. The vascularization of the explanted tumors was evaluated immunohistochemically using goat anti-CD31 antibodies (Santa Cruz Biotechnology Inc.).

RESULTS

Expression and Purification of hnTf-VEGF

Expression plasmid pPICZαB-hnTf-VEGF containing the genes encoding hnTf with the linker and $VEGF_{165}$ was constructed (Fig. 1). The plasmid was transformed into *P. pastoris* yeast and was cultured in induction medium

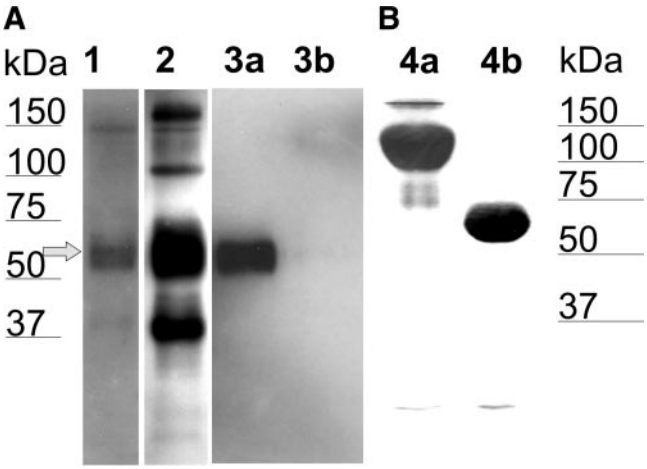

FIGURE 2. (A) SDS–PAGE of *P. pastoris* culture medium on a 10% Tris gel under reducing conditions followed by Western blot using antibodies against VEGF (lane 1), Tf (lane 2), or poly-His affinity tag (lane 3a). A protein with M_r of 65 kDa indicating hnTf-VEGF monomer was present in medium of clone KM71H transformed with pPICZαB-hnTf-VEGF (arrow) but not in medium of KM71H transformed with the parent pPICZαB vector (lane 3b). This protein was positive for VEGF and Tf. (B) SDS–PAGE of hnTf-VEGF purified by Co^{2+} metal affinity resin. The major band corresponded to hnTf-VEGF protein with M_r of 130 kDa (dimer) under nonreducing conditions (lane 4a) or M_r of 65 kDa (monomer) under reducing conditions (lane 4b).

(BMMY). The culture medium was analyzed by SDS–PAGE under reducing conditions and Western blot using polyclonal anti-VEGF (Fig. 2, lane 1), polyclonal anti-Tf (Fig. 2, lane 2), or monoclonal anti–poly-His (Fig. 2, lane 3a) antibody. The results showed a band corresponding to a protein with M_r of 65 kDa (hnTf-VEGF monomer) present only in the medium and not in the cell pellet (not shown). This band was absent in the medium of *P. pastoris* transformed with control plasmid pPICZαB (Fig. 2, lane 3b). The KM71H yeast strain was found to give the highest expression level of hnTf-VEGF 4 d after methanol induction. Large-scale expression and purification of hnTf-VEGF was performed. SDS–PAGE (10%) under reducing and nonreducing conditions showed that the final hnTf-VEGF protein was pure, with a major band corresponding to the M_r 130-kDa dimer or the M_r 65-kDa monomer (Fig. 2, lanes 4a and 4b, respectively) The hnTf-VEGF protein yield was 2.6 mg/L of yeast culture.

Endothelial Cell Proliferation Assay

hnTf-VEGF protein and VEGF exhibited equivalent growth-stimulatory effects on HUVECs, with the maximum increase in cell growth observed at a concentration of 0.5–1 nmol/L (Fig. 3). The growth of HUVECs treated with 0–2.7 nmol/L hnTf-VEGF or 0–2.2 nmol/L VEGF was increased 3-fold compared with that of untreated cells.

Evaluation of Receptor-Binding Properties by Flow Cytometry

Flow cytometric analysis of fluorescein-labeled hnTf-VEGF incubated with PAECs transfected with the VEGFR2

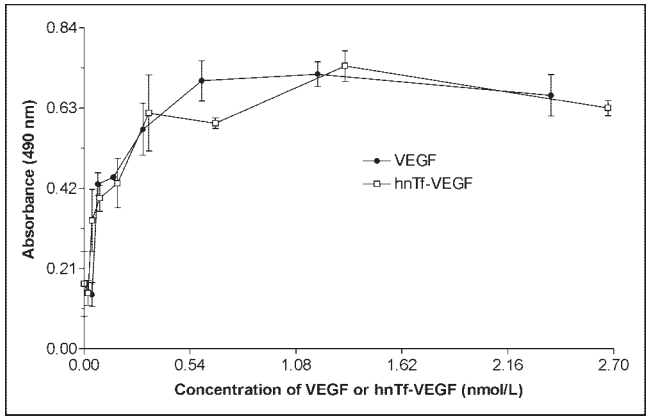

FIGURE 3. Effect of increasing concentrations of VEGF or hnTf-VEGF on growth of 5×10^3 HUVECs over a 72-h period measured colorimetrically using the CellTiter 96 AQueous One Solution proliferation assay.

gene demonstrated increased fluorescence. Binding to the cells was inhibited by a 50-fold molar excess of $VEGF_{165}$ (Fig. 4A) but not by a 50-fold excess of apotransferrin (Fig. 4B). There was no increased fluorescence when fluorescein-labeled hnTf-VEGF was incubated with control PAECs not transfected with VEGFR2 (not shown). These results indicated that hnTf-VEGF retained its ability to specifically bind VEGFR on PAECs but did not interact with transferrin receptors on the cells.

Radiolabeling of hnTf-VEGF with ^{111}In

hnTf-VEGF was labeled directly with ^{111}In through the hnTf moiety with an incorporation efficiency of 34% and was purified on a P-2 minicolumn to a final radiochemical purity >95% (Fig. 5). The specific activity of ^{111}In-hnTf-

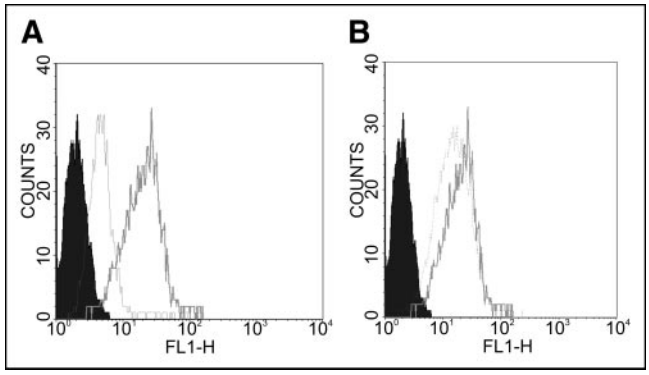

FIGURE 4. (A) Flow cytometry showing binding of fluorescein-conjugated hnTf-VEGF to PAECs transfected with the gene encoding VEGFR2 (KDR/flk-1) in the absence (solid line) or the presence (broken line) of a 50-fold excess of VEGF. (B) Binding of fluorescein-conjugated hnTf-VEGF to PAECs encoding VEGFR2 in the absence (solid line) or the presence (broken line) of a 50-fold excess of apotransferrin. The black-filled area in A and B represents cells not incubated with fluorescein-conjugated hnTF-VEGF or apotransferrin. There was no binding of hnTf-VEGF to PAECs that were not transfected with VEGFR2 (not shown).

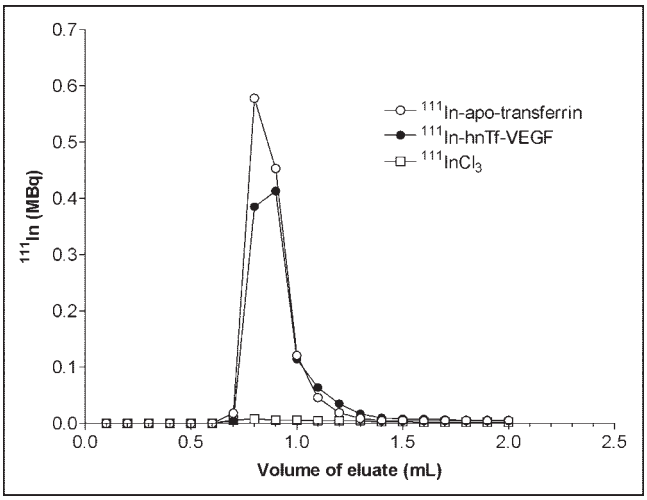

FIGURE 5. Size-exclusion chromatographic purification of ^{111}In-labeled hnTf-VEGF or apotransferrin (0.35 nmol) on a P-2 minicolumn eluted with 150 mmol/L sodium chloride. Radioactivity in each 100-μL fraction was measured in a radioisotope dose calibrator. The elution profile of free $^{111}InCl_3$, which does not elute from the column, is shown for comparison.

VEGF was 2.75×10^4 MBq/μmol. There was 7.5% ± 0.9% of ^{111}In eluting in the methanol fraction in Sep-Pak analysis of a sample of an 11-mer peptide [GGGGSHHHHHH] containing a C-terminal His_6 tag incubated with $^{111}InCl_3$ in 10 mmol/L HEPES/15 mmol/L $NaHCO_3$ buffer, pH 7.4, for 30 min compared with 5.6% ± 1.3% for buffer (without peptide) incubated with $^{111}InCl_3$ (not significantly different; *t* test, $P > 0.05$). These results indicated that the His_6 tag incorporated into hnTf-VEGF was unable to bind significant amounts of ^{111}In.

In Vitro Stability of ^{111}In-hnTf-VEGF

A moderate rate of loss of ^{111}In from ^{111}In-hnTf-VEGF to transferrin when incubated in vitro with human plasma at 37°C for up to 72 h was determined by size-exclusion HPLC (Table 1). The maximum cumulative loss of ^{111}In from ^{111}In-hnTf-VEGF over 72 h was 63.9% ± 1.3%; the mean daily rate of loss was 21.3% ± 3.4%. ^{111}In-hnTf-VEGF was stable to transchelation of ^{111}In when incubated with equimolar amounts of DTPA in 10 mmol/L HEPES/15 mmol/L $NaHCO_3$ buffer, pH 7.4, at 37°C for 4 h. Ultrafiltration analysis showed that 94.5% ± 0.6% of ^{111}In remained bound to hnTf-VEGF compared with that of ^{111}In-transferrin incubated with DTPA (92.9% ± 2.5%) for this same period (not significantly different; *t* test, $P > 0.05$).

Tumor and Normal Tissue Distributions

The tumor and normal tissue uptake of ^{111}In-hnTf-VEGF in athymic mice implanted subcutaneously with U87MG glioblastoma xenografts is shown in Table 2. The concentration of radioactivity in the blood decreased 2-fold from 3.6 ± 0.7 %ID/g at 48 h after injection to 1.6 ± 0.4 %ID/g at 72 h after injection. Tumor accumulation increased slightly over this same period from 5.9 ± 1.8 %ID/g to 6.7 ± 1.1 %ID/g, but the difference was not significant ($P > 0.05$). Tumor-to-blood ratios increased from 2.1 ± 0.05 at 48 h after injection to 4.9 ± 1.4 at 72 h after injection. The highest normal tissue concentrations of radioactivity at 72 h after injection were observed in the liver, kidneys, and spleen (45.5 ± 7.5, 39.3 ± 7.0, and 35.6 ± 4.4 %ID/g, respectively). The normal tissue distribution of ^{111}In-transferrin at 72 h after injection in a group of 3 athymic mice determined in a separate experiment was significantly different than that of ^{111}In-hnTf-VEGF at this point (Table 2).

Posterior, whole-body posterior images of athymic mice implanted with subcutaneous U87MG tumors at 24, 48, and 72 h after injection of ^{111}In-hnTf-VEGF are shown in Figure 6. Tumor uptake of radioactivity was evident at each time point but appeared to increase with time. High uptake of radioactivity was observed in the liver and kidneys. The tumor radioactivity was similar when mice were injected with ^{111}In-hnTf-VEGF combined with 100 times (in moles) the amount of apotransferrin (Fig. 6B), but tumors were not visualized when the radiopharmaceutical was combined with 100-fold molar excess of VEGF. Moreover, there was negligible whole-body retention of radioactivity in mice receiving ^{111}In-hnTf-VEGF combined with a 100-fold excess (in moles) of VEGF (images not shown), which was consistent with the tissue distribution results (Table 2). These findings were obtained in all mice studied in 2 independent experiments. U87MG tumors contained well-established tumor vasculature assessed by immunohistochemical staining using anti-CD31 antibodies (Fig. 6C).

DISCUSSION

In this study, we described a novel recombinant hnTf-VEGF protein that binds ^{111}In through the transferrin moiety without the need to introduce DTPA metal chelators. This protein interacts specifically with VEGFR but not with transferrin receptors on VECs. The hnTf-VEGF protein consisted of the n-lobe of human transferrin (hnTf) fused to the N-terminus of $VEGF_{165}$ through a flexible polypeptide linker [$(GGGGS)_3$]. The linker was inserted to avoid steric

TABLE 1
In Vitro Stability of ^{111}In-hnTf-VEGF Incubated with Human Plasma

Time (h)	^{111}In transchelated to transferrin from ^{111}In-hnTf-VEGF* (%)
0.25	2.8 ± 1.3
4	10.0 ± 0.4
24	27.9 ± 0.5
48	46.5 ± 5.2
72	63.9 ± 2.3

*Values are mean ± SE for triplicate determinations. ^{111}In-hnTf-VEGF was incubated with human plasma at 37°C for the specified times and the percentage transchelation to transferrin was measured by size-exclusion HPLC.

TABLE 2
Biodistribution of ^{111}In-hnTf-VEGF in Athymic Mice Bearing Subcutaneous U87MG Human Glioblastoma Xenografts

	%ID/g (mean ± SE)*				
	^{111}In-hnTf-VEGF		^{111}In-hnTf-VEGF + 100-fold molar excess of unlabeled Tf, 72 h	^{111}In-hnTf-VEGF + 100-fold molar excess of unlabeled VEGF,† 72 h	^{111}In-hTf,‡ 72 h
Tissue	48 h	72 h			
Blood	3.64 ± 0.73	1.61 ± 0.36§	2.15 ± 1.39	0.05 ± 0.02	0.78 ± 0.12
Heart	5.32 ± 2.18	4.69 ± 0.55	3.06 ± 0.22	0.12 ± 0.04	3.11 ± 1.14
Lung	10.91 ± 4.29	13.79 ± 0.73	8.05 ± 1.52¶	0.55 ± 0.16	24.16 ± 3.08
Liver	32.43 ± 0.08	45.53 ± 7.46	48.27 ± 3.20	3.89 ± 0.94	12.24 ± 1.54‖
Kidneys	26.41 ± 6.99	39.35 ± 7.02	23.29 ± 4.63	0.88 ± 0.31	15.70 ± 2.73‖
Spleen	26.05 ± 7.98	35.55 ± 4.36	12.98 ± 1.40¶	1.26 ± 0.44	7.66 ± 0.26‖
Stomach	1.26 ± 0.25	2.98 ± 0.50	1.40 ± 0.25	0.11 ± 0.01	1.71 ± 0.37
Intestines	5.65 ± 0.67	8.02 ± 0.53§	5.71 ± 1.42	0.35 ± 0.13	4.19 ± 0.50
Muscle	2.86 ± 0.96	3.80 ± 0.19	2.26 ± 0.71	0.15 ± 0.07	1.76 ± 0.06
Tumor	5.88 ± 1.84	6.68 ± 1.13	4.82 ± 1.26	0.42 ± 0.11	nd
Brain	1.64 ± 0.73	0.87 ± 0.03	0.60 ± 0.07¶	0.03 ± 0.01	0.65 ± 0.03

*Values are mean ± SE of cohorts of 3 or 4 mice.
†$P < 0.05$, comparison between ^{111}In-hnTf-VEGF with or without 100-fold molar excess of unlabeled VEGF at 72 h.
‡Biodistribution analysis for ^{111}In-hTf in normal organs was conducted as a separate experiment. nd = not determined.
§$P < 0.05$, comparison between 48 and 72 h.
¶$P < 0.05$, comparison between ^{111}In-hnTf-VEGF with or without 100-fold molar excess of unlabeled Tf at 72 h.
‖$P < 0.05$, comparison between ^{111}In-hnTf-VEGF and ^{111}In-hTf at 72 h.
Two-tailed Student *t* test with a 95% confidence interval was used to calculate statistical significance.

interference in the ability of the hnTf and $VEGF_{165}$ domains to bind to ^{111}In or VEGFR, respectively. The preservation of VEGFR binding by hnTf-VEGF was anticipated by its dimerization (M_r of 130 kDa) in solution required for receptor binding (*11*), which was detected by SDS–PAGE under nonreducing conditions (Fig. 2). SDS–PAGE under reducing conditions showed that the dimers dissociated into monomers (M_r of 65 kDa). hnTf-VEGF dimer binding to the VEGFR is critical for cell signaling (*12*).

The specific binding of fluorescein-labeled hnTf-VEGF to PAECs by flow cytometry (Fig. 4) confirmed that VEGFR binding was maintained. The displacement of binding of hnTf-VEGF protein to PAECs by a 50-fold molar excess of $VEGF_{165}$, but not by a 50-fold excess of apotransferrin, indicated that binding to endothelial cells was mediated by VEGFR and not by transferrin receptors. Preservation of binding properties of hnTf-VEGF to VEGFR was further demonstrated functionally by its growth-stimulatory effects on HUVECs similar to those of $VEGF_{165}$ (Fig. 3). The 3-fold increased growth rate of HUVECs exposed to 0.5–1 nmol/L of hnTf-VEGF or $VEGF_{165}$ compared with untreated cells was similar to that reported for $VEGF_{165}$ using a thymidine incorporation assay (*13,14*).

hnTf-VEGF was directly labeled with ^{111}In through the hnTf moiety. ^{111}In was not bound by the incorporated His_6 affinity tag, because an 11-mer peptide containing this se-

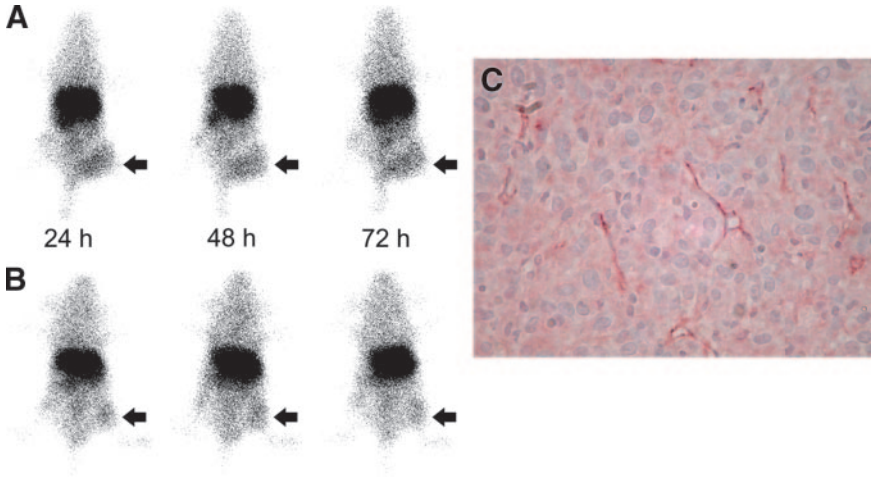

FIGURE 6. (A) Posterior whole-body images of a representative athymic mouse implanted subcutaneously with a U87MG glioblastoma xenograft in right hind leg (arrow) at 24, 48, and 72 h after injection of 2 MBq (5 μg) of ^{111}In-hnTf-VEGF. (B) Comparable images obtained by coadministration of a 100-fold excess (in moles) of unlabeled apotransferrin. Images obtained after administration of ^{111}In-hnTf-VEGF combined with a 100-fold excess (in moles) of unlabeled VEGF showed negligible whole-body retention of radioactivity at all time points (not shown). (C) Immunohistochemical staining of an explanted U87MG tumor using anti-CD31 antibodies shows positively staining blood vessel endothelial cells.

quence [GGGGSHHHHHH] was unable to bind significant amounts of ^{111}In. DTPA dianhydride, which reacts with the N-terminus or ϵ-amino groups of lysine amino acids on proteins, is the most commonly used bifunctional chelator for introducing DTPA groups into biomolecules. Derivatization of key lysines required for receptor recognition may, however, diminish receptor-binding affinity. $VEGF_{165}$ contains several lysines that are required for receptor binding. In particular, Lys-84 within the β5 loop is important for interaction with the receptor (*8*). DTPA derivatization of this residue may interfere with binding VEGFR. The hnTf-VEGF protein allowed labeling with ^{111}In at a site remote from the VEGFR-binding domain, thus preserving its ability to interact with VECs. A further advantage of including only the n-lobe in the protein is that, although either lobe can bind metal ions, binding to transferrin receptors requires the presence of both the n- and c-lobes (*9,10*). Therefore, the hnTf-VEGF protein only binds VEGFR and not transferrin receptors on VECs.

The dissociation constant (K_d) of hnTf-VEGF for ^{111}In was not measured. The binding of metal ions, such as indium by transferrin, is complicated and is dependent on many variables, including the concentration of the synergistic anion (e.g., HCO_3^-), pH, and salt concentration. Thus, the reported K_d values for binding of indium by transferrin have ranged widely from 10^{-19} mol/L to 10^{-30} mol/L (*15–17*). The K_d for binding ^{111}In by DTPA is 10^{-28} mol/L (*18*), but this value is for an octadentate complex. A heptadentate ^{111}In-DTPA complex is formed when one of the carboxylic acid groups is used for conjugation to proteins; this complex is less stable (*19*). Loss of ^{111}In from ^{111}In-DTPA–conjugated biomolecules in vivo is attributed to the 100-fold difference in the affinity between transferrin and ^{111}In, compared with DTPA and ^{111}In as well as the substantially greater concentration of transferrin in plasma (*20*). In our study, we similarly found that there was a moderate loss of ^{111}In from ^{111}In-hnTf-VEGF to transferrin in plasma in vitro over a 72-h period (21.3% ± 3.4% per day). This rate of transchelation of ^{111}In to transferrin is higher than reported for monoclonal antibodies labeled with ^{111}In through DTPA (8%–12% per day) (*19*). We speculate that this rate was caused by the high concentration of transferrin in plasma, which kinetically favored transchelation of ^{111}In from hnTf-VEGF, rather than caused by differences in ^{111}In binding affinity (since hnTf-VEGF incorporates one of the metal-binding sites of transferrin). ^{111}In-hnTf-VEGF was stable for transchelation to DTPA with <5% loss of ^{111}In over 4 h in vitro at 37°C.

^{111}In-hnTf-VEGF accumulated in highly vascularized U87MG glioblastoma xenografts in athymic mice, allowing imaging as early as 24 h after injection. The tumor uptake of ^{111}In-hnTf-VEGF was greatly reduced from 6.7 ± 1.1 %ID/g to 0.4 ± 0.1 %ID/g when coadministered with a 100-fold excess of unlabeled $VEGF_{165}$ (Table 2). It was not significantly reduced (4.8 ± 1.3 %ID/g) when combined with a 100-fold excess of apotransferrin. These results suggested that the tumor uptake of ^{111}In-hnTf-VEGF was mediated by VEGFR and not by transferrin receptors. Interestingly, coadministration of an excess of $VEGF_{165}$ (but not apotransferrin) drastically diminished retention of radioactivity not only in U87MG tumors but also in the blood and all other tissues examined (Table 2). The reason for the much more rapid elimination of ^{111}In-hnTf-VEGF from the blood and other tissues in the presence of an excess of $VEGF_{165}$ is not known, but these findings were reproducible in all mice in 2 independent studies and were visualized on images (not shown). One possible explanation is that inhibition of binding of ^{111}In-hnTf-VEGF to VEGFR by $VEGF_{165}$ on VECs may encourage its elimination from the body. Another possible explanation is that VEGF-mediated inhibition of the binding between ^{111}In-hnTf-VEGF and soluble VEGFR in the blood or interstitial fluid may promote elimination. Soluble VEGFR-1 (sFlt1) has been found in human serum and plasma (*21*), on macrophages and monocytes infiltrating tumors (*22,23*), and in many solid tumors, including breast cancer (*24*), renal cancer (*22*), and astrocytoma (*25*). The levels of sFlt-1 have been correlated with those of VEGF and may have an important role in tumor progression.

There was high uptake of radioactivity in the liver, kidneys, and spleen of athymic mice administered ^{111}In-hnTf-VEGF (45.5 ± 7.5, 39.4 ± 7.0, and 35.6 ± 4.4 %ID/g, at 72 h after injection, respectively; Table 2). This uptake was not diminished by coadministration of a 100-fold molar excess of apotransferrin but was reduced by coadministration of a 100-fold molar excess of VEGF. In contrast, the liver, kidney, and spleen uptakes of ^{111}In-transferrin in athymic mice were 3- to 5-fold significantly lower at 12.2 ± 1.5, 15.7 ± 2.7, and 7.7 ± 0.3 %ID/g, respectively (Table 1). Taken together, we believe that the liver and kidney uptakes of radioactivity were related to ^{111}In-hnTf-VEGF and not to loss of ^{111}In from the protein to transferrin with uptake of ^{111}In-transferrin in the tissues. Therefore, the transchelation of ^{111}In from ^{111}In-hnTf-VEGF to transferrin in plasma observed in vitro may not be representative of the extent of transchelation in vivo, because there is sequestration in vivo of ^{111}In-hnTf-VEGF by tumor and normal tissues and elimination from the blood, which diminishes the opportunity for transchelation of ^{111}In.

Despite the high liver, kidney, and spleen accumulations, our results suggest that ^{111}In-hnTf-VEGF may be useful for imaging angiogenesis in solid tumors mediated by the VEGF/VEGFR pathway. Other approaches to imaging VEGF/VEGFR-mediated angiogenesis have focused on radiolabeled antibodies directed against VEGFR or radiolabeled VEGF itself. ^{124}I-HuMV833 anti-VEGF monoclonal antibodies were used to image tumor angiogenesis in 20 patients by PET (*26*). PET was also used to image HT1080 human fibrosarcoma xenografts in mice using ^{124}I-labeled VG76e anti-VEGF monoclonal antibodies (*27*). Lu et al. (*28*) derivatized $VEGF_{121}$ site specifically with maleimide-modified DTPA at Cys-116 and labeled it with ^{111}In for imaging angiogenesis in ischemic muscle in rabbits. Derivatization with DTPA decreased the affinity of $VEGF_{121}$ for

binding KDR 2-fold in a competition assay and moderately diminished its growth-stimulatory effect on HUVECs. However, in a direct binding assay against KDR coated onto wells in a microplate, there was no decrease in receptor-binding affinity of ^{111}In-VEGF$_{121}$. These results (*28*) and our findings suggest that modification of VEGF at a site remote from its receptor-binding domain results in good preservation of receptor binding and function. Cornelissen et al. (*29*) imaged angiogenesis in athymic mice implanted with A2058 human melanoma xenografts using ^{123}I-VEGF$_{165}$. Tumors were successfully visualized and the tumor uptake of ^{123}I-VEGF$_{165}$ was significantly reduced by coadministration of 80 μg of unlabeled VEGF$_{165}$. Li et al. (*30,31*) imaged gastrointestinal tumors and metastases as well as pancreatic carcinoma in patients using ^{123}I-VEGF$_{165}$. ^{111}In-hnTf-VEGF offers advantages over radioiodinated VEGF by avoiding the problems of in vivo deiodination and redistribution of radioiodine, which were observed in these studies (*29–31*).

CONCLUSION

A novel recombinant hnTf-VEGF fusion protein was expressed in *P. pastoris*. The protein bound ^{111}In directly through the transferrin moiety without the need to introduce DTPA metal chelators. ^{111}In-hnTf-VEGF interacted specifically with VEGFR on VECs but not with transferrin receptors. ^{111}In-hnTf-VEGF localized avidly and specifically in angiogenic U87MG human glioblastoma xenografts in athymic mice, allowing tumor imaging at 72 h after injection. We conclude that ^{111}In-hnTf-VEGF is a promising radiopharmaceutical for imaging VEGFR-mediated angiogenesis in solid tumors.

ACKNOWLEDGMENTS

This research was supported by grants from the Natural Sciences and Engineering Research Council of Canada (Strategic Grant 182945), U.S. Army Breast Cancer Research Program (Concept Award BC995715), and the Canadian Breast Cancer Research Alliance (grant 016456). The authors are grateful to the Biologic Resources Branch of the U.S. National Cancer Institute for the supply of recombinant human VEGF. Parts of this study were presented at the Third Annual Meeting of the Society for Molecular Imaging in St. Louis, MO, September 9–12, 2004.

REFERENCES

1. Hanahan D, Folkman J. Patterns and emerging mechanisms of the angiogenic switch during tumorigenesis. *Cell.* 1996;86:353–364.
2. Berkman RA, Merrill MJ, Reinhold WC, et al. Expression of the vascular permeability factor/vascular endothelial growth factor gene in central nervous system neoplasms. *J Clin Invest.* 1993;91:153–159.
3. Speirs V, Atkin SL. Production of VEGF and expression of the VEGF receptors Flt-1 and KDR in primary cultures of epithelial and stromal cells derived from breast tumours. *Br J Cancer.* 1999;80:898–903.
4. Plate KH, Breier G, Millauer B, Ullrich A, Risau W. Up-regulation of vascular endothelial growth factor and its cognate receptors in a rat glioma model of tumor angiogenesis. *Cancer Res.* 1993;53:5822–5827.
5. Vajkoczy P, Farhadi M, Gaumann A, et al. Microtumor growth initiates angiogenic sprouting with simultaneous expression of VEGF, VEGF receptor-2, and angiopoietin-2. *J Clin Invest.* 2002;109:777–785.
6. Folkman J. Tumor angiogenesis: therapeutic implications. *N Engl J Med.* 1971; 285:1182–1186.
7. Hsei V, Deguzman GG, Nixon A, Gaudreault J. Complexation of VEGF with bevaczumab decreases VEGF clearance in rats. *Pharm Res.* 2002;19:1753–1756.
8. Keyt BA, Nguyen HV, Berleau LT, et al. Identification of vascular endothelial growth factor determinants for binding KDR and FLT-1 receptors: generation of receptor-selective VEGF variants by site-directed mutagenesis. *J Biol Chem.* 1996;271:5638–5646.
9. Mason AB, Tam BM, Woodworth RC, et al. Receptor recognition sites reside in both lobes of human serum transferrin. *Biochem J.* 1997;326:77–85.
10. Zak O, Trinder D, Aisen P. Primary receptor-recognition site of human transferrin is in the C-terminal lobe. *J Biol Chem.* 1994;269:7110–7114.
11. Potgens AJ, Lubsen NH, van Altena MC, et al. Covalent dimerization of vascular permeability factor/vascular endothelial growth factor is essential for its biological activity: evidence from Cys to Ser mutations. *J Biol Chem.* 1994;269:32879–32885.
12. Fuh G, Li B, Crowley C, Cunningham B, Wells JA. Requirements for binding and signaling of the kinase domain receptor for vascular endothelial growth factor. *J Biol Chem.* 1998;273:11197–11204.
13. Hewett PW, Murray JC. Coexpression of flt-1, flt-4 and KDR in freshly isolated and cultured human endothelial cells. *Biochem Biophys Res Commun.* 1996;221: 697–702.
14. Mohanraj D, Olson T, Ramakrishnan S. A novel method to purify recombinant vascular endothelial growth factor (VEGF121) expressed in yeast. *Biochem Biophys Res Commun.* 1995;215:750–756.
15. Harris WR, Chen Y, Wein K. Equilibrium constants for the binding of indium(III) to human serum transferrin. *Inorg Chem.* 1994;31:4991–4998.
16. Lurie DJ, Smith FA, Shukri A. The dissociation of some ^{111}In chelates in the presence of transferrin and haemoglobin studied by PAC. *Int J Appl Radiat Isot.* 1985;36:57–62.
17. Kulprathipanja S, Hnatowich DJ, Beh R, and Elmaleh D. Formation constants of gallium- and indium-transferrin. *Int J Nucl Med Biol.* 1979;6:138–141.
18. Welch MJ, Welch TJ. Solution chemistry of carrier-free indium. In: Subramanian G, Rhodes BA, Cooper JF, Sodd J, eds. *Radiopharmaceuticals*. New York, NY: Society of Nuclear Medicine;1975:73–79.
19. Reilly R, Lee N, Houle S, Law J, Marks A. In vitro stability of EDTA and DTPA immunoconjugates of monoclonal antibody 2G3 labeled with indium-111. *Int J Rad Appl Instrum [A].* 1992;43:961–967.
20. Cole WC, DeNardo SJ, Meares CF, et al. Comparative serum stability of radiochelates for antibody radiopharmaceuticals. *J Nucl Med.* 1987;28:83–90.
21. Barleon B, Reusch P, Totzke F, et al. Soluble VEGFR-1 secreted by endothelial cells and monocytes is present in human serum and plasma from healthy donors. *Angiogenesis.* 2001;4:143–154.
22. Harris AL, Reusch P, Barleon B, Hang C, Dobbs N, Marme D. Soluble Tie2 and Flt1 extracellular domains in serum of patients with renal cancer and response to antiangiogenic therapy. *Clin Cancer Res.* 2001;7:1992–1997.
23. Sawano A, Iwai S, Sakurai Y, et al. Flt-1, vascular endothelial growth factor receptor 1, is a novel cell surface marker for the lineage of monocyte-macrophages in humans. *Blood.* 2001;97:785–791.
24. Toi M, Bando H, Ogawa T, Muta M, Hornig C, Weich HA. Significance of vascular endothelial growth factor (VEGF)/soluble VEGF receptor-1 relationship in breast cancer. *Int J Cancer.* 2002;98:14–18.
25. Lamszus K, Ulbricht U, Matschke J, Brockmann MA, Fillbrandt R, Westphal M. Levels of soluble vascular endothelial growth factor (VEGF) receptor 1 in astrocytic tumors and its relation to malignancy, vascularity, and VEGF-A. *Clin Cancer Res.* 2003;9:1399–1405.
26. Jayson GC, Zweit J, Jackson A, et al. Molecular imaging and biological evaluation of HuMV833 anti-VEGF antibody: implications for trial design of antiangiogenic antibodies. *J Natl Cancer Inst.* 2002;94:1484–1493.
27. Collingridge DR, Carroll VA, Glaser M, et al. The development of [^{124}I]iodinated-VG76e: a novel tracer for imaging vascular endothelial growth factor in vivo using positron emission tomography. *Cancer Res.* 2002;62:5912–5919.
28. Lu E, Wagner WR, Schellenberger U, et al. Targeted in vivo labeling of receptors for vascular endothelial growth factor: approach to identification of ischemic tissue. *Circulation.* 2003;108:97–103.
29. Cornelissen B, Oltenfreiter R, Kersemans V, et al. In vitro and in vivo evaluation of [^{123}I]-VEGF$_{165}$ as a potential tumor marker. *Nucl Med Biol.* 2005;32:431–436.
30. Li S, Peck-Radosavljevic M, Kienast O, et al. Iodine-123-vascular endothelial growth factor-165 (^{123}I-VEGF$_{165}$). Biodistribution, safety and radiation dosimetry in patients with pancreatic carcinoma. *Q J Nucl Med Mol Imaging.* 2004;48:198–206.
31. Li S, Peck-Radosavljevic M, Kienast O, et al. Imaging gastrointestinal tumours using vascular endothelial growth factor-165 (VEGF$_{165}$) receptor scintigraphy. *Ann Oncol.* 2003;14:1274–1277.